Nonlinear Control and Optimization of the Burn Condition in Tokamak Nuclear Fusion Reactors

Mark D. Boyer and Eugenio Schuster

Abstract— **The ITER tokamak, the next experimental step in the development of nuclear fusion reactors, will explore the burning plasma regime in which temperature is sustained mostly by fusion heating. Control of the fusion power through modulation of fueling and heating sources, referred to as burn control, will be essential for achieving and maintaining desired operating points and ensuring stability. We utilize a spatially averaged nonlinear transport model to design a multi-variable nonlinear burn control strategy that can reject large perturbations and move between operating points. The controller uses the available actuation techniques in tandem to ensure good performance, even if one or more of the actuators saturate. We propose the use of a model-based optimization scheme to drive the system to a state that minimizes a given cost function. A simulation study shows the performance of the control scheme with a cost function weighting fusion power and temperature tracking errors.**

I. Introduction

For nuclear fusion to become an economical energy source, tokamak reactors must be capable of operating for long periods of time in a burning plasma mode characterized by a large fusion gain, the ratio of fusion power to auxiliary power. Achieving and maintaining such conditions will require precise control over the plasma density and temperature. Due to the nonlinear and coupled dynamics of the system, modulation of the burn condition without a well designed control scheme could result in undesirable transient performance. Feedback control will also be necessary for responding to unexpected changes in plasma confinement, impurity content, or other parameters. Furthermore, certain conditions can lead to thermal instabilities. In any of these situations, disruptive plasma instabilities could be triggered, stopping operation and potentially damaging the machine.

In past work, the feasibility of potential actuators has been studied. Prior work, including [1], [2], [3], considered modulation of auxiliary power, fueling rate, and controlled injection of impurities as possible actuators. Most existing efforts use just one of these actuators and linearize the system model to use linear control design techniques. In [4], a diagonal multi-input, multi-output linear control scheme was developed for controlling burning plasmas. Non-model-based proportional-integral control was studied in [5]. When tested using nonlinear models, these control strategies stabilize the system against a limited set of perturbations. In our previous work [6], a zero-dimensional nonlinear model involving approximate conservation equations for the energy and the densities of the ion species was used to design a nonlinear feedback controller for stabilizing the density and energy of the plasma. The controller utilized all of the actuators simultaneously, using auxiliary power modulation to prevent quenching, impurity injection to increase radiation losses and stop thermal excursions, and fueling modulation to regulate density. Nonlinear burn control using multiple actuators had only been done previously using non-model-based techniques, like neural networks [7]. The use of nonlinear control techniques removed the operability limits imposed by linearization in other works.

Despite the advantages of the nonlinear controller designed in [6] over previous designs, the use of impurity injection could lead to undesirable accumulation of impurity ions within the plasma core, which could reduce the efficiency of the reactor long after thermal excursions are rejected. As an alternative to impurity injection, we introduced a nonlinear controller exploiting the dependence of the fusion power on the fraction of tritium in the deuterium-tritium plasma as a means of altering fusion heating [8]. Such an approach is made possible through independent control of deuterium and tritium fuel sources, a technique called isotopic fuel tailoring [9]. By combining this technique with modulation of auxiliary heating, control of the burn condition can be maintained, even when the auxiliary power saturates, without resorting to impurity injection. While the use of isotopic fueling to control plasma heating is a promising tool for burn control, its usefulness may be limited to some extent due to particle recycling. In this process, particles lost from the plasma strike the walls of the reactor are reflected or re-emitted back to the plasma and act as a refueling source. This decrease the dependence of the tritium fraction on the controlled fuel injection, slowing response time. We study this effect through the addition of particle recycling to the model and overcome the possible limitations by utilizing impurity injection as a back-up actuator. We include a model-based optimization scheme, similar to the approach for general nonlinear systems used in [10], to drive the system to a state that minimizes a given cost function.

The plasma model is given in Section II. Control objectives and an online optimization scheme are described in Section III. In Section IV, the control algorithm is presented. Section V shows the results of a simulation study. Finally, the conclusions and future plans are given in Section VI.

II. Burning plasma model

We use a volume averaged model for a burning plasma employing approximate energy and particle balance equations.

This work was supported by the NSF CAREER award program (ECCS-0645086). M. D. Boyer (m.dan.boyer@lehigh.edu), and E. Schuster are with the Department of Mechanical Engineering and Mechanics, Lehigh University, Bethlehem, PA 18015, USA.

We consider deuterium and tritium ion densities separately and include an approximate model of particle recycling. The particle and energy balance equations are given by

$$\dot{n}_\alpha = -\frac{n_\alpha}{\tau_\alpha^*} + S_\alpha \quad (1)$$

$$\dot{n}_D = -\frac{n_D}{\tau_D} + f_{eff} S_D^R - S_\alpha + S_D^{inj} \quad (2)$$

$$\dot{n}_T = -\frac{n_T}{\tau_T} + f_{eff} S_T^R - S_\alpha + S_T^{inj} \quad (3)$$

$$\dot{n}_{I,c} = -\frac{n_{I,c}}{\tau_I^*} + S_I^{inj} \quad (4)$$

$$\dot{n}_{I,sp} = -\frac{n_{I,sp}}{\tau_I^*} + S_I^{sp} \quad (5)$$

$$\dot{E} = -\frac{E}{\tau_E} + P_\alpha - P_{rad} + P_{aux} + P_{Ohm} \quad (6)$$

where n_α, n_D, n_T, and E are the α-particle, deuterium, tritium, and energy densities, respectively. The term $n_{I,c}$ represents the density of impurities from controlled impurity injection, while $n_{I,sp}$ represents the impurity density arising due to sputtering from plasma facing components of the confinement vessel. The confinement times for respective quantities are denoted as τ_α^*, τ_D, τ_T, τ_I^*, and τ_E. The particle confinement times are assumed to scale with the energy confinement time, i.e.

$$\tau_\alpha^* = k_\alpha^* \tau_E, \;\; \tau_D = k_D \tau_E, \;\; \tau_T = k_T \tau_E, \;\; \tau_I^* = k_I^* \tau_E \quad (7)$$

where k_α^*, k_D, k_T, and k_I^* are constants. In this work, the α-particle and impurity particle balances use effective confinement times chosen to account for the effects of recycling, while confinement times for deuterium and tritium do not, as deuterium-tritium recycling is modeled separately. The source of α-particles from fusion is given by

$$S_\alpha = \gamma (1-\gamma) n_{DT}^2 \langle \sigma v \rangle \quad (8)$$

$$n_{DT} = n_D + n_T \quad (9)$$

$$\gamma = \frac{n_T}{n_{DT}} \quad (10)$$

where n_{DT} is the density of deuterium-tritium fuel and γ is the tritium fraction. The DT reactivity $\langle \sigma \nu \rangle$ is a highly nonlinear, positive and bounded function of the plasma temperature, T, and is calculated by

$$\langle \sigma \nu \rangle = exp\left(\frac{a}{T^r} + a_2 + a_3 T + a_4 T^2 + a_5 T^3 + a_6 T^4\right) \quad (11)$$

where the parameters a_i and r are taken from [11].

The terms S_D^{inj} and S_T^{inj} (controller inputs) are the deuterium and tritium injection rates, respectively and the terms S_D^R and S_T^R represent the fluxes due to particle recycling.The model of deuterium and tritium recycling used here is based on the following description. Upon leaving the plasma and reaching the vessel walls, a fraction f_{ref} (typically $0.2 \leq f_{ref} \leq 0.9$) of the exiting particles may be reflected back towards the plasma, while the remainder are either absorbed by the wall material (an effect called wall pumping), or removed from the vessel by the active pumping system. The wall pumping effect causes the development of a inventory of particles in the wall, which is, over time, re-emitted back to the confinement vessel. To avoid the need for a complex model of wall conditions and active pumping efficiency, the amount of recycling from the plasma facing surfaces can be characterized by a global recycling coefficient $R^{eff} = S^R/S^S$ (typically $R^{eff} > 0.6$), where S^R is the recycled particle flux and S^S is the particle flux to the plasma facing surfaces. The wall inventory, and consequently the re-emitted particles, will have some tritium fraction, which we denote γ^{PFC}. The recycled (reflected or re-emitted) particles go on to fuel the plasma core with some efficiency, f_{eff}, depending on their energy and interaction with the plasma boundary. The fraction of particles that is 'screened' by the boundary returns to the plasma facing surface again to be either reflected, absorbed, or pumped out [12]. Based on this description, we can derive the following expressions for the recycled flux:

$$S_D^R = \frac{1}{1 - f_{ref}(1 - f_{eff})} \left\{ f_{ref} \frac{n_D}{\tau_D} + \left(1 - \gamma^{PFC}\right) \times \left[\frac{\left(1 - f_{ref}(1 - f_{eff})\right) R^{eff}}{1 - R^{eff}(1 - f_{eff})} - f_{ref} \right] \left(\frac{n_D}{\tau_D} + \frac{n_T}{\tau_T} \right) \right\}$$

$$S_T^R = \frac{1}{1 - f_{ref}(1 - f_{eff})} \left\{ f_{ref} \frac{n_T}{\tau_T} + \gamma^{PFC} \times \left[\frac{\left(1 - f_{ref}(1 - f_{eff})\right) R^{eff}}{1 - R^{eff}(1 - f_{eff})} - f_{ref} \right] \left(\frac{n_D}{\tau_D} + \frac{n_T}{\tau_T} \right) \right\}$$

The term S_I^{inj} (controller input) is the injection of impurities used to increase the controlled impurity density $n_{I,c}$ to cool the plasma. We model the sputtering source as

$$S_I^{sp} = \frac{f_I^{sp} n}{\tau_I^*} + f_I^{sp} \dot{n}$$

where $0 \leq f_I^{sp} \ll 1$ in order to maintain $n_{I,sp} = f_I^{sp} n$ where n is the total plasma density. This simple model reflects the fact that there is typically a small uncontrolled impurity content in the plasma. To simplify presentation of the controller design, both impurity populations have the same effective confinement time τ_I^*, and atomic number Z_I. Total impurity content $n_I = n_{I,s} + n_{I,c}$ is then governed by

$$\dot{n}_I = -\frac{n_I}{\tau_I^*} + S_I^{inj} + S_I^{sp} \quad (12)$$

P_{aux} (controller input) represents the auxiliary heating power, while $P_\alpha = Q_\alpha S_\alpha$ is the plasma heating from fusion where $Q_\alpha = 3.52$ MeV is the energy of α-particles. P_{rad} represents the radiative cooling losses, which are approximated by the expression for bremsstrahlung losses used in [13], i.e.,

$$P_{rad} = A_{brem}\left(n_D + n_T + 4n_\alpha + Z_I^2 n_I\right) n_e \sqrt{T(keV)} \quad (13)$$

where A_{brem} is a constant and n_e is the electron density. The electron density is obtained from the neutrality condition $n_e = n_D + n_T + 2n_\alpha + Z_I n_I$. The plasma density and temperature are

$$n = n_\alpha + n_D + n_T + n_I + n_e = 2n_D + 2n_T + 3n_\alpha + (Z_I + 1) n_I \quad (14)$$

$$T = \frac{2}{3}\frac{E}{n} \quad (15)$$

Ohmic heating P_{Ohm} is approximated by

$$P_{Ohm} = 2.8 \times 10^{-9} \frac{Z_{eff} I^2}{a^4 T^{3/2}} \quad (16)$$

where I is in Amps and T is in keV [13]. We use the energy confinement scaling [14]

$$\tau_E = f_\tau I_p^{0.93} B_T^{0.15} P^{-0.69} n_{e19}^{0.41} M^{0.19} R^{1.97} \epsilon^{0.58} \kappa_{95}^{0.78} \quad (17)$$

where $f_\tau = 0.0562$, $I_p = 15.0MA$ is the plasma current, $B_T = 5.3T$ is the toroidal magnetic field, $P = P_{aux} + P_{Ohm} + P_\alpha - P_{rad}$ is the total power (MW), n_{e19} is the electron density ($10^{19}\mathrm{m}^{-3}$), M is the effective mass of the plasma (amu), $R = 6.2m$ is the major radius, $\epsilon = a/R$ with $a = 2.0m$ the minor radius, and $\kappa_{95} = 1.7$ is the elongation at the 95% flux surface/separatrix.

For the control design, we consider the states of the burning plasma system to be n_α, n_I, E, γ, and n. The dynamic equations for the first three have already been given in (1), (4), and (6), while, by noting (9), (10), and (14), the remaining two equations can be written as

$$\begin{aligned}\dot{\gamma} = &-\frac{\gamma}{\tau_T} + \frac{\gamma(1-\gamma)}{\tau_D} + \frac{\gamma^2}{\tau_T} \\ &+ \frac{2}{n - 3n_\alpha - (Z_I+1)n_I} \Big\{ f_{eff} S_T^R - S_\alpha + S_T^{inj} \\ &-\gamma \left[f_{eff}\left(S_D^R + S_T^R\right) - 2S_\alpha + S_D^{inj} + S_T^{inj} \right] \Big\} \quad (18)\end{aligned}$$

$$\begin{aligned}\dot{n} = &2\left[-\frac{n - 3n_\alpha - (Z_I+1)n_I}{2} \left(\frac{1-\gamma}{\tau_D} + \frac{\gamma}{\tau_T} \right) \right. \\ &\left. + f_{eff}\left(S_D^R + S_T^R\right) - 2S_\alpha + S_D^{inj} + S_T^{inj} \right] \\ &+ 3\left[-\frac{n_\alpha}{\tau_\alpha^*} + S_\alpha \right] + (Z_I+1)\left[-\frac{n_I}{\tau_I^*} + S_I^{inj} + S_I^{sp} \right] \quad (19)\end{aligned}$$

III. Control Objectives

The steady-state operating points of the system can be determined by solving the nonlinear algebraic equations obtained by setting the left-hand side of (1), (4), (6), (18), and (19) to zero. Considering only operating points for which no impurities are injected, i.e., $S_I^{inj} = 0$, $n_{I,c} = 0$, a unique solution to this system of equations is obtained by specifying references n^r, γ^r, and E^r. We note that $n_{I,c} = 0$ is stable without controlled impurity injection, and the steady-state density of alpha-particles associated with the selected operating point can be shown to be input-to-state stable with respect to the references. We consider the first objective of the control scheme to be the selection of an operating point in such a way that a particular cost function is minimized. We consider a convex (at least locally in the domain of interest) cost function $p(r,x)$ that weights a combination of steady-state plasma parameters associated with a particular reference $r = [E^r, n^r]$ and states $x = [\gamma, n_I]^T$. The reference r will be modified online to minimize $p(r,x)$ for a given value of x. The states x will be used as virtual actuators in the control design and n_α cannot be chosen independently at steady-state, so these states are not considered as degrees of freedom in the optimization. Following an approach similar to the one used in [10], we take as the Lyapunov function $V_r = \frac{1}{2}\left(\frac{\partial p(r,x)}{\partial r}\right)^T \frac{\partial p(r,x)}{\partial r}$. By taking the time derivative of V_r, we obtain

$$\dot{V}_r = \left(\frac{\partial p}{\partial r}\right)^T \left[\frac{\partial^2 p}{\partial r^2}\dot{r} + \frac{\partial^2 p}{\partial r \partial x}\dot{x} \right]$$

We can then choose as an update law

$$\dot{r} = -\left(\frac{\partial^2 p}{\partial r^2}\right)^{-1} \left[K_{RTO}\frac{\partial p}{\partial r} + \frac{\partial^2 p}{\partial r \partial x}\dot{x} \right]$$

where K_{RTO} is diagonal and positive definite, leading to

$$V_r \le -\left(\frac{\partial p}{\partial r}\right)^T K_{RTO} \frac{\partial p}{\partial r}$$

This implies that $\frac{\partial p}{\partial r} \to 0$ and, therefore, r is driven toward the optimal x-dependent set point, r^*.

In this work, we consider the goal of regulating the fusion heating $\bar{P}_\alpha^r$ and plasma temperature $\bar{T}^r$ at steady-state, i.e., we minimize the cost function

$$p(r,x) = \frac{1}{2}\left(\bar{P}_\alpha(r,x) - \bar{P}_\alpha^r\right)^2 + \frac{R_p}{2}\left(\bar{T}(r,x) - \bar{T}^r\right)^2 \quad (20)$$

where $\bar{P}_\alpha(r,x)$ and $\bar{T}(r,x)$ are the steady-state fusion power and temperature associated with r and x. R_p is used to weight the relative importance of the temperature. We can write the dynamics of the error variables $\tilde{E} = E - E^r$, $\tilde{n} = n - n^r$, and $\tilde{\gamma} = \gamma - \gamma^r$ as

$$\dot{\tilde{E}} = -\frac{\tilde{E}}{\tau_E} - \frac{E^r}{\tau_E} + P_\alpha - P_{rad} + P_{Ohm} + P_{aux} - \dot{E}^r \quad (21)$$

$$\dot{\tilde{\gamma}} = -\frac{\tilde{\gamma}}{\tau_T} + \frac{2\left[u + (1-\gamma)S_T^{inj} - \gamma S_D^{inj}\right]}{n - 3n_\alpha - (Z_I+1)n_I}$$

$$\dot{\tilde{n}} = -\tilde{n}\left(\frac{1-\gamma}{\tau_D} + \frac{\gamma}{\tau_T}\right) + v - \dot{n}^r + 2\left(S_T^{inj} + S_D^{inj}\right) \quad (22)$$

where

$$\begin{aligned}u(\gamma^r) = &\frac{n - 3n_\alpha - (Z_I+1)n_I}{2}\left[-\frac{\gamma^r}{\tau_T} + \frac{\gamma(1-\gamma)}{\tau_D} + \frac{\gamma^2}{\tau_T} - \dot{\gamma}^r \right] \\ &+ f_{eff}S_T^R - S_\alpha - \gamma\left[f_{eff}\left(S_D^R + S_T^R\right) - 2S_\alpha\right] \quad (23)\end{aligned}$$

$$\begin{aligned}v = &\left(-n^r + 3n_\alpha + (Z_I+1)n_I\right)\left(\frac{1-\gamma}{\tau_D} + \frac{\gamma}{\tau_T}\right) \\ &+ 2\left[f_{eff}\left(S_D^R + S_T^R\right) - 2S_\alpha\right] + 3\left[-\frac{n_\alpha}{\tau_\alpha^*} + S_\alpha\right] \\ &+ (Z_I+1)\left[-\frac{n_I}{\tau_I^*} + S_I^{inj} + S_I^{sp}\right] \quad (24)\end{aligned}$$

The objective of the controller designed in the following section is to ensure the stability of the origin for this dynamic system, thereby guaranteeing that the system tracks the operating point that minimizes the cost function p.

IV. Controller Design

We note that $\tilde{E}$ can be driven to zero by satisfying

$$f(n, E, n_\alpha, n_I, \gamma) = -\frac{E^r}{\tau_E} + P_{Ohm} + P_\alpha - P_{rad} + P_{aux} - \dot{E}^r = 0 \quad (25)$$

The condition (25) can be satisfied in several different ways. The auxiliary heating term P_{aux} enters the equation directly, the actuators S_D^{inj} and S_T^{inj} can be used to change the α-heating term P_α by modulating the tritium fraction, and the impurity injection term S_I^{inj} can be used to increase the impurity content and consequently P_{rad}. Having several methods for controlling the energy subsystem enables us to design a control scheme that can still achieve stabilization despite saturation some of the available actuators.

Step 1: We first calculate the P_{aux} as

$$P_{aux} = \frac{E^r}{\tau_E} - Q_\alpha \gamma^r (1-\gamma^r)\, n_{DT}^2 \langle\sigma v\rangle + P_{rad} - P_{Ohm} + \dot{E}^r \tag{26}$$

subject to the limit P_{aux}^{max}, which depends on installed power on the machine, and the limit $P_{aux}^{min} \geq 0$ depends on the operating scenario. For example, some minimum power may be needed to maintain the required amount of non-inductive current drive during a particular discharge since some sources of power also serve as sources of plasma current.

Step 2: We next find a trajectory γ^* satisfying (25), i.e.,

$$Q_\alpha \gamma^* (1-\gamma^*)\, n_H^2 \langle\sigma\nu\rangle - P_{rad} + P_{Ohm} + P_{aux} = \frac{E^r}{\tau_E} + \dot{E}^r \tag{27}$$

Solving this equation yields

$$\gamma^* (1-\gamma^*) = \frac{\frac{E^r}{\tau_E} + P_{rad} - P_{Ohm} + P_{aux} + \dot{E}^r}{Q_\alpha n_H^2 \langle\sigma\nu\rangle} = C \tag{28}$$

$$\gamma^* = \frac{1 \pm \sqrt{1-4C}}{2} \tag{29}$$

Note that, if the value of P_{aux} calculated in Step 1 is not saturated, then $\gamma^* = \gamma^r$. This can be shown by substituting (26) into (27). If $C \leq 0.25$, the two resulting solutions for γ^* are real and we take the tritium-lean solution, such that $\gamma^* \leq 0.5$. If $C \geq 0.25$, even the optimal isotopic mix and maximum value of auxiliary heating will not generate enough heating to satisfy $f = 0$, indicating that the requested operating point may not be achievable for the amount of auxiliary heating power installed on the device. Barring this situation, based on our choice of P_{aux} and γ^*, we have that

$$f(n, E, n_\alpha, n_I, \gamma^*) = 0 \tag{30}$$

This allows us to write $f = \hat{\gamma}\phi_\gamma$ where $\hat{\gamma} = \gamma - \gamma^*$ and ϕ_γ is a continuous function. Noting (21), (25), we can then write the dynamics of the energy perturbation as

$$\dot{\tilde{E}} = -\frac{\tilde{E}}{\tau_E} + \hat{\gamma}\phi_\gamma \tag{31}$$

and the dynamics of $\hat{\gamma}$ can be written as

$$\dot{\hat{\gamma}} = -\frac{\hat{\gamma}}{\tau_T} + \frac{2\left[u(\gamma^*) + (1-\gamma) S_T^{inj} - \gamma S_D^{inj}\right]}{n - 3n_\alpha - (Z_I+1)\, n_I} \tag{32}$$

Step 3: Having selected P_{aux} and γ^* in the previous steps, we choose S_D^{inj} and S_T^{inj} to ensure $\tilde{E}$, $\hat{\gamma}$, and $\tilde{n}$, which are governed by (31), (32), and (22), are driven to zero. We consider the Lyapunov function $V_0 = V_n + V_{E,\gamma}$ where $V_n = \frac{1}{2}\tilde{n}^2$ and $V_{E,\gamma} = \frac{1}{2}k_1\tilde{E}^2 + \frac{1}{2}\hat{\gamma}^2$. Satisfying the conditions

$$2\left(S_T^{inj} + S_D^{inj}\right) = -v + \dot{n}^r - K_n\tilde{n} \tag{33}$$

$$(1-\gamma) S_T^{inj} - \gamma S_D^{inj} = -\frac{n - 3n_\alpha - (Z_I+1)\, n_I}{2} \times \left(k_1\tilde{E}\phi_\gamma + K_\gamma\hat{\gamma}\right) - u(\gamma^*) \tag{34}$$

where $K_n > 0$ and $K_\gamma > 0$ results in

$$\dot{V}_n = -\tilde{n}^2\left(\frac{1-\gamma}{\tau_D} + \frac{\gamma}{\tau_T} + K_n\right) < 0 \tag{35}$$

$$\dot{V}_{E,\gamma} = -k_1\frac{\tilde{E}^2}{\tau_E} - \left(\frac{1}{\tau_T} + K_\gamma\right)\hat{\gamma}^2 < 0 \tag{36}$$

such that $\dot{V}_0 < 0$, guaranteeing asymptotic stability of the system. Conditions (33) and (34) can be satisfied by choosing

$$S_D^{inj} = \frac{n - 3n_\alpha - (Z_I+1)\, n_I}{2}\left(k_1\tilde{E}\phi_\gamma + K_\gamma\hat{\gamma}\right) + u(\gamma^*) + (1-\gamma)\left(\frac{-v - K_n\tilde{n}}{2}\right) \tag{37}$$

$$S_T^{inj} = \left(\frac{-v - K_n\tilde{n}}{2}\right) - S_D^{inj} \tag{38}$$

These values are subject to the constraints $0 \leq S_D^{inj} \leq S_D^{inj,max}$ and $0 \leq S_T^{inj} \leq S_T^{inj,max}$. If one of the fueling actuators saturate, we cannot satisfy both conditions of the control law, so we must choose to either control n or γ. We maintain control of the density by satisfying (33).

If, due to actuator saturation, $\dot{V}_{E,\gamma} > 0$, we cannot ensure stability of the burn condition with the previously considered actuators. There are two possible situations to consider, either a thermal quench or an excursion. If the system is experiencing a quench, the controller has already increased auxiliary heating to its maximum, so the only alternative would be to change the magnetic plasma parameters to improve energy confinement (see (17)) or to change the reference operating point to one that is achievable. If the system is experiencing a thermal excursion, however, we can use impurity injection to stabilize the energy subsystem, despite the heating and fueling actuator saturation. In these cases we enable the use of impurity injection by setting the flag $F_{imp} = 1$ and proceed to Step 4.

Step 4: If $F_{imp} = 1$, we use the expression for radiation losses given in (13) to find an impurity density trajectory n_I^* that satisfies condition (25). Defining the error $\hat{n}_I = n_I - n_I^*$, we can write its dynamics as

$$\dot{\hat{n}}_I = -\frac{\hat{n}_I}{\tau_I^*} - \frac{n_I^*}{\tau_I^*} + S_I^{inj} + S_I^{sp} - \dot{n}_I^* \tag{39}$$

Based on the choice of n_I^*, we have that

$$f(n, E, n_\alpha, \gamma, n_I^*) = 0 \tag{40}$$

which allows us to write $f = \hat{n}_I\phi_I$ where ϕ_I is a continuous function. We can then rewrite (21) as

$$\dot{\tilde{E}} = -\frac{\tilde{E}}{\tau_E} + \hat{n}_I\phi_I \tag{41}$$

We take as a Lyapunov function $V_1 = V_n + V_\gamma + V_{E,I}$ where $V_\gamma = \frac{1}{2}\hat{\gamma}^2$ and $V_{E,I} = \frac{1}{2}k_3\tilde{E}^2 + \frac{1}{2}\hat{n}_I^2$. By satisfying

$$S_I^{inj} = -k_3\tilde{E}\phi_I + \frac{n_I^*}{\tau_I^*} - S_I^{sp} + \dot{n}_I^* - K_I\hat{n}_I \quad (42)$$

where $K_I > 0$, the derivative of $V_{E,I}$ can be reduced to

$$\dot{V}_{E,I} = -k_3\frac{\tilde{E}^2}{\tau_E} - \left(K_I + \frac{1}{\tau_I}\right)\hat{n}_I^2 < 0 \quad (43)$$

We modify the tritium fraction trajectory to $\gamma^* = \gamma^*_{\text{(Step 2)}} - K_S\int_{t_0}^{t} S_I^{inj}dt$ where $\gamma^*_{\text{(Step 2)}}$ is the value of γ^* calculated in Step 2, $K_S > 0$, and t_0 is the time at which impurity injection was first engaged. This modification ensures that the tritium fraction is, if possible, eventually reduced to such a level that impurity injection is no longer needed, i.e., $S_I^{inj} \to 0$. Once $S_I^{inj} = 0$, we disable impurity injection in subsequent executions of the algorithm by setting $F_{imp} = 0$. By satisfying

$$2\left(S_T^{inj} + S_D^{inj}\right) = -v + \dot{n}^r - K_n\tilde{n} \quad (44)$$

$$(1-\gamma)S_T^{inj} - \gamma S_D^{inj} = -\frac{n - 3n_\alpha - (Z_I+1)n_I}{2}K_\gamma\hat{\gamma} - u(\gamma_I^*) \quad (45)$$

we ensure $\dot{V}_n < 0$, $\dot{V}_\gamma < 0$, and $\dot{V}_1 < 0$, guaranteeing stability. Conditions (44) and (45) are satisfied by

$$S_D^{inj} = \frac{n - 3n_\alpha - (Z_I+1)n_I}{2}K_\gamma\hat{\gamma} + u(\gamma^*) + (1-\gamma)\left(\frac{-v - K_n\tilde{n}}{2}\right) \quad (46)$$

$$S_T^{inj} = \left(\frac{-v - K_n\tilde{n}}{2}\right) - S_D^{inj} \quad (47)$$

which are subject to constraints. If a fueling actuator saturates, we again choose to hold (44) to stabilize the density.

V. Simulation Results

In the following simulation, references E^r and n^r were arbitrarily initialized and modified online to minimize the cost function p. The reference $\gamma^r = 0.5$ was kept constant throughout the simulation. The references for fusion heating and temperature, $\bar{P}_\alpha^r$ and $\bar{T}^r$, which enter into the cost function, were modified at $t = 60s$ and $t = 120s$ to show the ability of the scheme to move the system between operating points. The simulation considered a fractional content of impurities from sputtering of 2%, i.e., $f_I^{sp} = 0.02$, and the atomic number of the impurity species was taken to be $Z_I = 4$. The confinement scaling parameters were taken to be $k_\alpha^* = 7$, $k_D = k_T = 3$, and $k_I^* = 10$. We considered an installed heating power $P_{aux}^{max} = 73$ MW with the additional constraint $P_{aux}^{min} = \frac{5}{7}P_{aux}^{max}$. The recycling model parameters used were $\gamma^{PFC} = 0.5$, $f_{eff} = 0.3$, $f_{ref} = 0.5$, and $R^{eff} = 0.95$, representing unfavorable conditions for tritium fraction control. These parameters were selected to ensure impurity injection was required during the simulation to illustrate all aspects of the control scheme. Actual recycling parameters in ITER may be more favorable for control.

Results of the simulation are shown in Figure 1. Fusion heating and temperature, the components of the cost function (20), are shown in Figures 1a and 1b, while system states E, n, and γ are depicted in Figures 1c, 1d and 1e. The fractional content of alpha-particles and impurities are shown in Figure 1f and the actuators are given in Figures 1g and 1h. The initial operating point did not match the requested fusion heating and temperature and the optimization scheme immediately began to adjust the references E^r and n^r to reduce the error. Due to the initial conditions of the system, a significant reduction in heating was required to track the reference E^r at $t = 0$, causing the auxiliary power to saturate. In order to achieve the necessary reduction in heating, the requested tritium fraction trajectory γ^* was reduced, however, the unfavorable particle recycling conditions in the simulation caused the fueling actuators to saturate and the actual tritium fraction could not track the request. To overcome this, impurity injection was enabled to cool the plasma. Impurity content increased for a short time until around $t = 10s$, at which point, due to the increasing reference E^r, additional auxiliary heating was required and impurity injection was disabled. The tritium fraction then returned to its reference value and the impurity content decayed back to its nominal level $f_I = f_I^{sp} = 0.02$. By around $t = 40s$, the scheme successfully forced the system to the optimal operating point, achieving the desired fusion heating and temperature. At $t = 60s$ the requested fusion heating and temperature were changed and the optimization scheme adjusted the references E^r and n^r accordingly. These requests were successfully tracked by the nonlinear control scheme by reducing heating and fueling, and the desired fusion heating and temperature were achieved by around $t = 100s$. At $t = 120s$, the references were changed again. The reference E^r was driven down significantly by the optimization scheme and, as a result, auxiliary power saturated at its minimum. The request γ^* was reduced and, although the actual tritium fraction began to follow the request this time, impurity injection was still needed to cool the plasma initially. By around $t = 150s$, the tritium fraction reached the requested value γ^* and impurity injection was disabled. At about the same time, the fusion heating and temperature reached the desired values and the controller regulated the system throughout the remainder of the simulation. The fractional content of impurities decayed to its intrinsic level $f_I = f_I^{sp} = 0.02$ and the alpha particle content converged to its steady-state value.

VI. Conclusions

We have presented a nonlinear model of a burning tokamak plasma including a simplified model of the effects of particle recycling on density dynamics and proposed a nonlinear control and model-based extremum seeking scheme for optimizing the burn condition for a given cost function. The nonlinear controller combines modulation of the auxiliary power and fueling sources with impurity injection to ensure performance and stability even when one or more actuators saturate. Future work will include combining this scheme

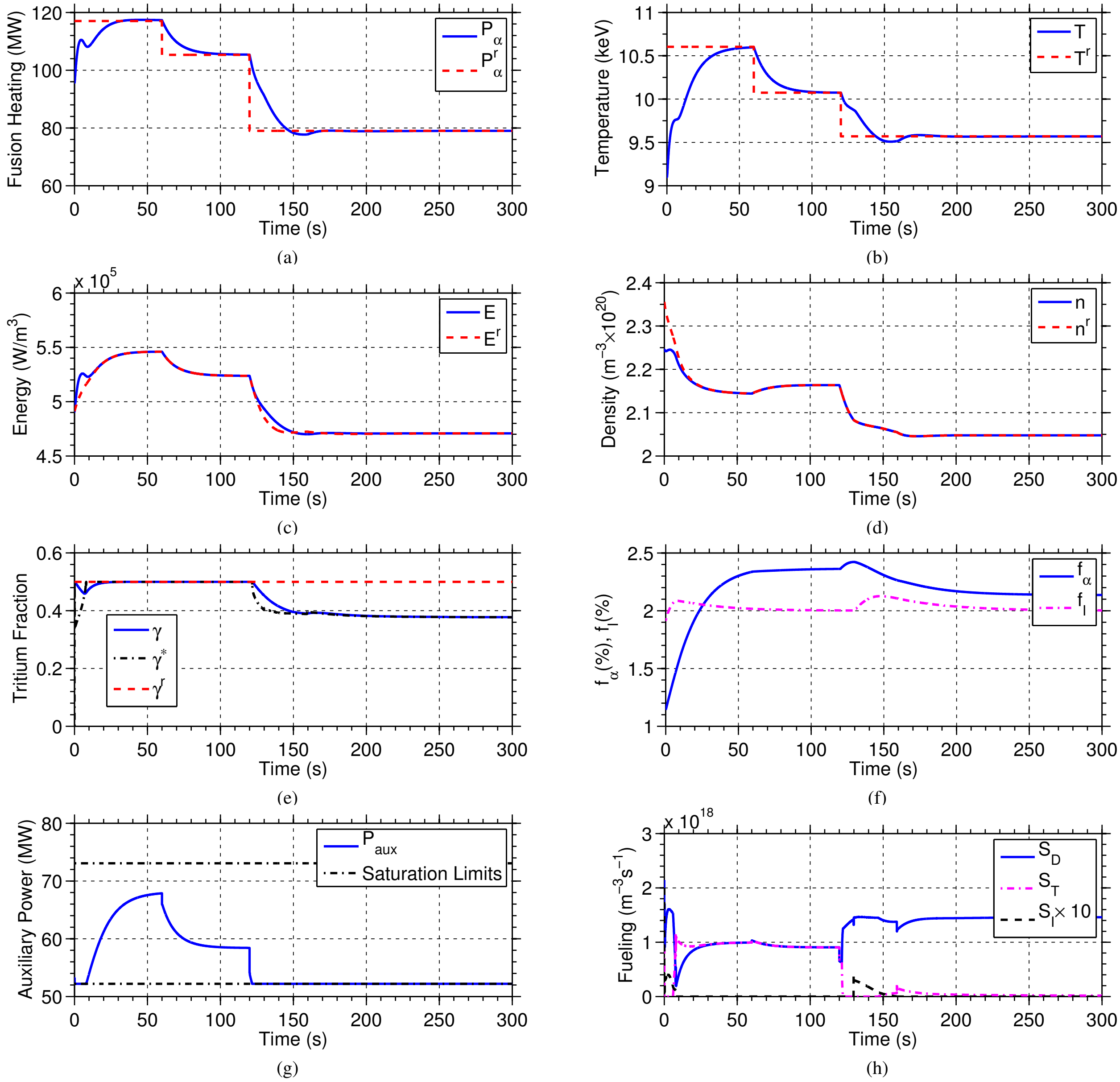

Fig. 1: Closed loop evolution of (a) fusion heating, (b) temperature, (c) energy, (d) density, (e) tritium fraction, (f) alpha-fraction, and impurity fraction, along with closed loop response of (g) auxiliary heating and (h) fueling actuators.

with the adaptive control strategy we employed in [15] and considering constraints in the optimization scheme.

REFERENCES

[1] J. Mandrekas and W. M. Stacey, "Evaluation of Different Burn Control Methods for the International Thermonuclear Experimental Reactor," *13th IEEE Symp. on Fusion Eng.*, vol. 1, pp. 404–407, 1989.

[2] S. W. Haney, Perkins, and Others, "Active Control of Burn Conditions for the International Thermonuclear Experimental Reactor," *Fusion Tech.*, vol. 18, no. 4, pp. 606–17, 1990.

[3] D. Anderson, T. Elevant, H. Hamen, M. Lisak, and H. Persson, "Studies of Fusion Burn Control," *Fusion Tech.*, vol. 23, no. 1, 1993.

[4] V. M. Leonov, Y. V. Mitrishkin, and V. E. Zhogolev, "Simulation of Burning ITER Plasma in Multi-Variable Kinetic Control System," in *32nd EPS Conference on Plasma Physics*, vol. 29, pp. 2–5, 2005.

[5] O. Mitarai, A. Sagara, R. Sakamoto, N. Ohyabu, A. Komori, and O. Motojima, "High-Density, Low Temperature Ignited Operations in FFHR," *Plasma and Fusion Research*, vol. 5, pp. S1001–S1001, 2010.

[6] E. Schuster, M. Krstić, and G. Tynan, "Burn Control in Fusion Reactors Via Nonlinear Stabilization Techniques," *Fusion Sci. and Tech.*, vol. 43, 2003.

[7] J. E. Vitela, "Burn Conditions Stabilization with Artificial Neural Networks of Subignited Thermonuclear Reactors with Scaling Law Uncertainties," *Plasma Phys. and Cont. Fusion*, vol. 43, 2001.

[8] M. Boyer and E. Schuster, "Zero-dimensional nonlinear burn control using isotopic fuel tailoring for thermal excursions," in *IEEE Conf. on Control Applications*, pp. 246–251, IEEE, 2011.

[9] L. R. Baylor, P. Parks, *et al.*, "Pellet Fuelling and Control of Burning Plasmas in ITER," *Nuclear Fusion*, vol. 47, pp. 443–448, 2007.

[10] M. Guay and T. Zhang, "Adaptive extremum seeking control of nonlinear dynamic systems with parametric uncertainties," *Automatica*, vol. 39, no. 7, 2003.

[11] L. Hively, "Special Topic Convenient Computational Forms For Maxwellian Reactivities," *Nuclear Fusion*, vol. 17, no. 4, p. 873, 1977.

[12] J. Ehrenberg, "Wall effects on particle recycling in tokamaks," in *Physical processes of the interaction of fusion plasmas with solids*, p. 35, Academic Press, 1996.

[13] W. M. Stacey, *Fusion: An Introduction to the Physics and Technology of Magnetic Confinement Fusion*. Wiley-VCH, 2nd ed., 2010.

[14] "Summary of the ITER final design report," tech. rep., IAEA, 2001.

[15] M. Boyer and E. Schuster, "Adaptive Nonlinear Burn Control in Tokamak Fusion Reactors," in *2012 American Controls Conf.*, 2012.